RSC Advances

ROYAL SOCIETY OF CHEMISTRY

www.rsc.org/advances

Morphology, mechanical, dielectric properties and rheological behavior of EAGMA toughed microcellular PEI/EAGMA foam

Yajie Lei, Tao Liu*, Zhenglei Chen, Ai Lu, Xianzhong Wang, Xiuli Zhao*

Institute of Chemical Materials, China Academy of Engineering Physics, Mianyang 621900, P. R. China

Abstract: A series of toughened polyetherimide (PEI)/ethylene-acrylate-glycidyl methacrylate copolymer (EAGMA) blends were prepared by twin screw extruder and then injection molded by conventional and microcellular methods. The effect of EAGMA content on the mechanical, thermal, dielectric properties, rheology behavior and morphology of PEI/EAGAM blends were investigated. The results shown that the PEI/EAGMA blends exhibited notched charpy impact strength of 27.9 KJ/m^2 which is 4~5 times higher than that of pure PEI and indicated that EAGMA had excellent toughening effect in the PEI/EAGMA system. The interface tension calculation and SEM photograph indicated that the PEI matrix had great compatibility with EAGMA elastomer. The rheological results shown the restriction in molecular mobility of PEI was more significant with the increasing content of EAGMA. Moreover, the dielectric constant and loss of the materials can be effectively reduced through the technology of micro-foaming, EAGAM plays an important role in the microcellular structure formation and final dielectric property of PEI/EAGMA foam.

Key Words: polymers; composites; microcellular injection molding; foam; toughness;

*Corresponding author: Tel.: +86 0816 2491421; Fax: +86 0816 2495856.
E-mail address: liutaocaep@hotmail.com (Tao Liu) or zhlx75@163.com (Xiuli Zhao).

1. Introduction

Microcellular foam is defined as having average cell sizes in the range of 1-10μm, and cell densities on the order of 10^9-10^{15} cells/cm^3. The microcellular foam was invented at the Massachusetts Institute of Technology (MIT) under the direction of Professor Nam P. Suh [1,2] and has been studied extensively for the past 20 years[3-5]. Because of its high strength-to-weight ratio, excellent heat and sound insulations, high energy or mass absorption and materials saving properties the microcellular foams have attracted significant attention [6-14]. Polyetherimide (PEI) is one of the most important high-performance engineering thermoplastics which is extensive used in commercial applications due to its excellent thermal stability, remarkable tensile strength, electrical insulating property, wear-resisting property, dimensional stability and flame resistance etc. However, so far there are a few investigations on microcellular foams which based on PEI [15-18] and according to the researches, most microcellular foams based on PEI were prepared by batch foaming method but have a lack of papers on the research of microcellular injection molding method. Nemoto et al. [18] prepared microcellular poly (ether ether ketone) (PEEK)/para-diamine poly (ether imide) (p-PEI) and PEEK/meta-diamine poly (ether imide) (m-PEI) foams, and found that the difference in chemical configuration between m- and p-PEI gave rise to a prominent change in the cell structure of the respective foams. Miller et al. [16, 17] investigated the micro-scale cells or nano-scale cells of PEI can be created by means of controlling the CO_2 pressure and the glass transition temperature of PEI at 5 MPa CO_2 pressure was lowered to 95 ^oC from

215 ^{o}C at normal atmosphere. Meanwhile, they found that nanofoams shown a significantly higher strain to failure, resulting in an improvement in the modulus of toughness by up to 350 % compared to microcellular foams.

Moreover, the rigid structure of PEI molecular chain leads to poor resistance to notched impact strength. For the reason, polymer blending has been usually applied as a facile method to solve the problem. Thus, a variety of polymers have been fully miscible with PEI matrix, such as poly (ether etherketone) [19-29], poly (ethylene naphthalate) [22,30-32], poly (butylene terephthalate) [33-35], poly (ethylene terephthalate) [36,37] polyarylate [38,39], poly (ether sulfone) [40] and polyamide 66 [41] etc. Although a lot of literatures reported the mechanical behavior of various PEI/polymer unfoamed blends in detail, very little attention was paid to the elastomer toughened PEI microcellular foams.

In this article, a series of toughened PEI/EAGMA blends were prepared by twin screw extruder. The PEI/EAGAM blends and foams were injection molded by conventional and microcellular method respectively. The effect of EAGMA content on mechanical, thermal, dielectric, cell properties, rheology behavior and morphology of PEI/EAGAM blends or foams were investigated.

2. Materials and experimental

2.1. Materials

PEI (Ultem 1100) was applied by Sabic, America. It is an amorphous thermoplastic with a measured density of 1.24 g/cm^3. EAGMA (AX 8900) was supplied by Arkema Inc, France. The molecular weight of PEI and EAGMA is 3.2×10^4 g/mol and 8×10^4

g/mol respectively.

2.2. PEI/EAGMA blends preparation

The PEI resin was firstly dried at 140 ^{o}C for 6 h to remove residual moisture and then mixed with EAGMA elastomer and processed in a PTW252 twin-screw extruder (HAAKE, Germany) to give samples. The rotational speed of the extruder was 120 rpm, and the temperatures of its eight sections, from the charging hole to the ram head, were 310, 320, 330, 330, 335, 330, 320, and 325 ^{o}C. The samples were dried at 120 ^{o}C for 8 h to remove moisture and then conventionally injected to standard testing samples.

2.3. Microcellular PEI/EAGMA foams preparation

Microcellular PEI/EAGMA foams were prepared by A VC 330H/80L injection molding machine (Engel, Austria) using supercritical nitrogen (SC-N2) as foaming agent. The supercritical fluid supply system was SII-TR-10 model (Trexel, America). The parameters of microcellular injection were shown in Table 1

2.4. Characterization

2.4.1 Mechanical properties

The tensile and flexural properties of samples were carried out with a CMT 7015 Material Test Instrument (SUNS, China) according to ISO 527-5: 1997, ISO 178: 1993, relatively. The crosshead speed for both tensile and flexural measurements was 5 mm/min. The notched charpy impact testing of samples was carried out with a PTM 1100 Material Test Instrument (SUNS, China) according to ISO 179-1:2000. All tests were carried out in air-conditioned room (25 ^{o}C).

2.4.2 Rheological characterization

Viscoelastic characterization of the blends was conducted with RS600 rotational rheometer (HAAKE, Germany). The linear viscoelastic range of deformation was obtained by a strain sweep test. The response to applied oscillatory deformation at 330 ^{o}C was evaluated in the frequency range of 0.01 to 100 Hz.

2.4.3 Thermal properties

The HDT(heat deflection temperature) of PEI/EAGMA blends were determined according to the standard of ISO 75-1: 2004. A load of 1.80 MPa was placed on each specimen, and the temperature was increased at 2 ^{o}C/min until the specimen deflect 0.32 mm. The dynamic thermomechanical (DMA) behavior of PEI/EAGMA blends with various EAGMA contents was studied using a Thermomechanical Analyzer, RSA3. The experiments were carried out using the three-point bending mode. PEI, EAGMA and PEI/EAMGA blends were carried out in the temperature range from -50 to 300°C with a heating rate of 3°C/min. All the tests were carried out at a frequency of 1 Hz and a strain level of 0.1%. TGA thermograms of the PEI/EAGMA blends with various EAGMA contents were determined by TA Instruments TGA-Q50 thermogravimetric analyzer with a heating rate of 20 ^{o}C/min from room temperature to 800 ^{o}C under nitrogen atmosphere.

2.4.4 SEM observations

The morphology of solid blends and foams was observed with a CamScan Apollo 300 scanning electron microscope (SEM). The cell density (N_f) - number of cells per cubic centimeter of the foams was calculated by Eq. (1)[42,43]:

$$N_f = (\frac{n}{A})^{3/2}(\frac{1}{1-V_f}) \quad (1)$$

Where n is the number of cells on the SEM micrograph, A the area of the micrograph (cm^2), and V_f the void fraction of the foamed sample, which can be estimated as:

$$V_f = 1 - \frac{\rho_f}{\rho} \quad (2)$$

Where ρ and ρ_f were the mass densities of solid and foamed samples, respectively.

2.4.5 Dielectric constant measurememts

The dielectric constant of both unfoamed and foamed samples was carried out with a 4292A precision impedance analyzer (Agilent, America). All the tests were carried out in the frequency range of 50 Hz~30 MHz under room temperature.

2.4.6 Contact angle measurements

Contact angles were measured in a sessile drop mold with DSA100 (Krüss, German). PEI and EAGMA samples were injected to testing samples with a Minijet 2 microscale injection molding machine (Thermofisher, America). Contact angles were measured on 3 μl wetting solvent at 25 ^{o}C.

3. Results and discussion

3.1 Blends morphology

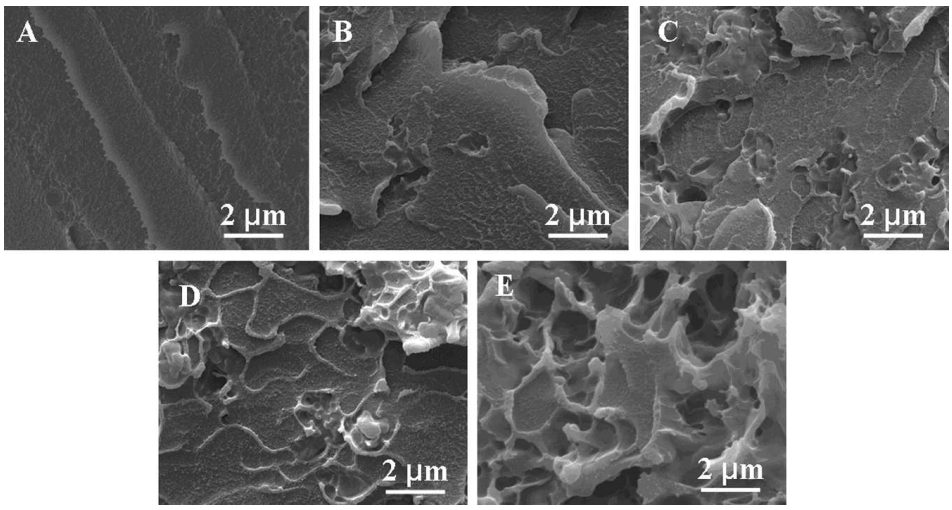

Fig.1. SEM micrographs of PEI/EAGMA blends. (A) PEI/EAGMA=100/0; (B) PEI/EAGMA=95/5; (C) PEI/EAGMA=90/10; (D) PEI/EAGMA=85/15; (E) PEI/EAGMA=80/20.

To understand the relationship between the properties and the phase morphology is necessary for material design. As shown in Fig.1, the interface between EAGMA elastomer and PEI matrix is very obscure and no sea-island morphology observed. The result indicates that there is a good compatibility between PEI and EAGMA. Moreover, the fracture surfaces of PEI/EAGMA blends reflected different degree of plastic deformation and tearing behavior. These are compelling proof of toughness increase with the increasing EAGMA content.

3.2 Interfacial tension

The interfacial tension is a key factor in study the formation of phase structure between EAGMA elastomer and PEI matrix. The processing parameters of microcellular injection molding process are listed in Table 1. The contact angles of different materials with water and diiodomethane are listed in Table 2 and the surface tension, dispersion, polar components of materials were calculated by Eqs. (3) and (4) [44].

$$(1+\cos\theta_{H_2O})\gamma_{H_2O} = 4\left(\frac{\gamma^d_{H_2O}\gamma^d}{\gamma^d_{H_2O}+\gamma^d} + \frac{\gamma^p_{H_2O}\gamma^p}{\gamma^p_{H_2O}+\gamma^p}\right) \quad (3)$$

$$(1+\cos\theta_{CH_2I_2})\gamma_{CH_2I_2} = 4\left(\frac{\gamma^d_{CH_2I_2}\gamma^d}{\gamma^d_{CH_2I_2}+\gamma^d} + \frac{\gamma^p_{CH_2I_2}\gamma^p}{\gamma^p_{CH_2I_2}+\gamma^p}\right) \quad (4)$$

$$\gamma_{12} = \gamma_1 + \gamma_2 - 4\left(\frac{\gamma^d_1\gamma^d_2}{\gamma^d_1+\gamma^d_2} + \frac{\gamma^p_1\gamma^p_2}{\gamma^p_1+\gamma^p_2}\right) \quad (5)$$

In the formula above, γ is the surface tension, γ^d is the dispersion component, γ^p is the polar component and θ is the contact angle with water or diiodomethane. γ_{12} is the interfacial tension between materials 1 and 2, γ_1 and γ_2 are the surface tensions of the two contacting components in the blends.

Tab. 1. Processing parameters of microcellular injection molding

Parameters	Value
Injection temperature (^{o}C)	330
Shot size (mm)	49
Content of SC-N_2 (wt %)	0.4
Injection speed (mm/s)	20
Mould temperature (^{o}C)	120

Table 2. The contact angle and surface tension of the polymers.

Sample	Contact angle (^{o})		Surface tension (mN/m)		
	Water	Diiodomethane	Total (γ)	Dispersion component (γ^d)	Polar component (γ^p)
PEI	76.02	23.98	57.56	46.66	10.90
EAGMA	81.07	32.2	52.70	43.58	9.12

The interfacial tension of PEI/EAGMA blend which calculated by the equation of Wu (Eq.(5)) [44] is very small, only 0.27 mN/m. According to the rule that the smaller interfacial tension of blends is, the better compatibility of blends is, in the PEI/EAGMA system, PEI matrix and EAGMA elastomer have a good compatibility, which is consistent with the morphology of PEI/EAGMA blends as seen in Fig.1.

3.3 Rheologic behavior

Dynamic strain sweeps at 330 °C is obtained in order to determine the linear viscoelastic region (LVR), and the data is displayed in Fig.2. According to the results of LVR, the response to applied oscillatory deformation at 330 °C is evaluated in the frequency range of 0.01 to 100 Hz at a strain of 100%.

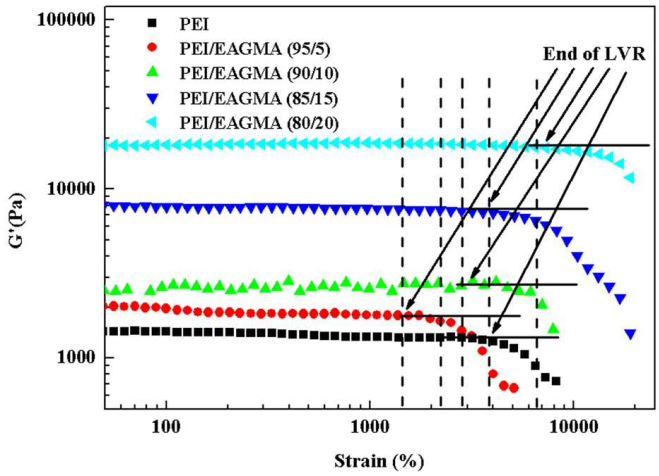

Fig.2. Comparison of linear viscoelastic region of the different samples at 330 °C.

Fig.3 shows the relationship between dynamic viscosity and frequency of PEI matrix and PEI/EAGMA blends. It is to seen that the dynamic viscosity of PEI/EAGMA blends decreases with the increasing of frequency which indicating PEI/EAGMA blends are obviously pseudoplastic fluid. Meanwhile, the dynamic viscosity of PEI/EAGMA blends increases remarkably with the increment of EAGMA

in low frequency region. This phenomenon was due to the higher dynamic viscosity of EAGMA. The EAGMA elastomer is elastic, so the motion of molecular chain of PEI will be hindered in the PEI/EAGMA blends.

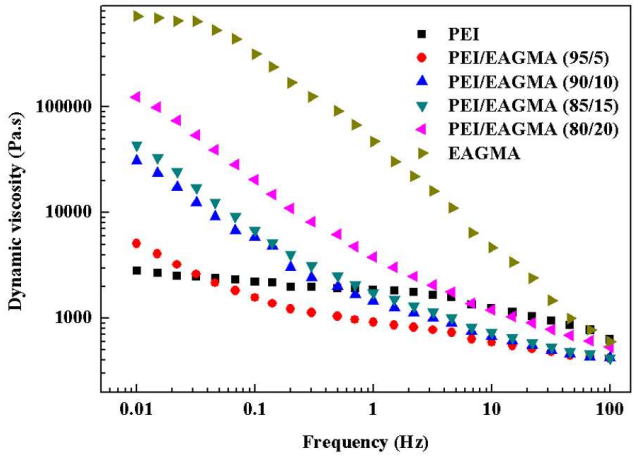

Fig.3. Comparison of the dynamic viscosity of the different samples at 330 ^{o}C.

Fig.4 and Fig.5 show the storage modulus G' and loss modulus G'' with frequency for PEI/EAGMA blends. The G' and G'' exhibits similar trend. At low frequency region, the G' of PEI/EAGMA blends increases with increasing EAGMA content which is related to the melt elasticity enhancement. The stronger the hydrodynamic effect in the melt, the more is the upturn of modulus as evidenced by relevant graphs in Fig.4 [45], whereas at high frequency region, G' of PEI/EAGMA blends decreases and lower than PEI matrix.

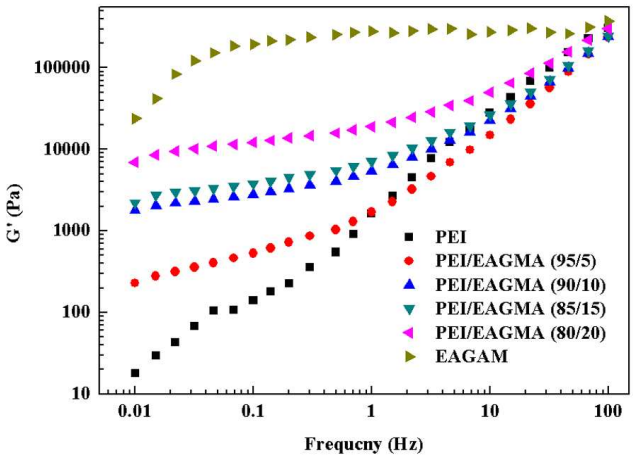

Fig.4. Comparison of the storage modulus curves of the different samples at 330 ^{o}C.

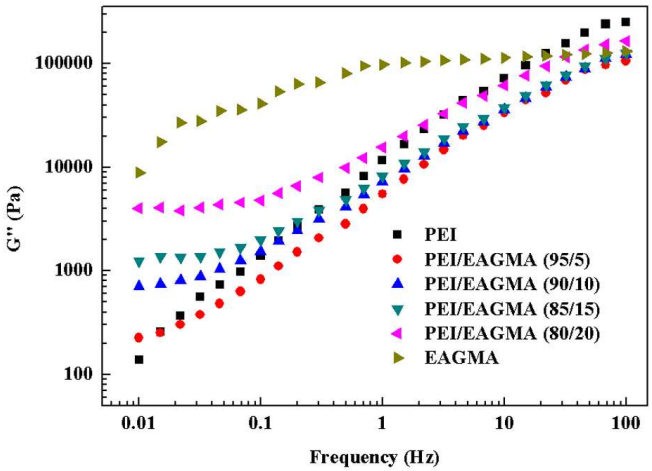

Fig.5. Comparison of the loss modulus curves of the different samples at 330 ^{o}C

The restricted molecular mobility can also be traced by crossover point characteristic at which the values of G' and G'' are equal. By increasing the angular frequencies, the crossover point indicates a transition from viscous deformation to elastic behavior. The shift in crossover frequency represents the changes in molecular mobility and relaxation time behavior. As seen in Fig.6, the crossover frequency of blends decreases with the increasing EAGMA content. This may due to the influence

of EAGMA on the molecular mobility of PEI matrix. EAGAM is a kind of elastomer with high viscosity, the molecular chain of EAGMA is more difficult to move than PEI. Therefore, the mobility of PEI molecular chain will be restricted by the incorporation of EAGMA. Meanwhile the restriction in molecular mobility is more significant with the increasing EAGMA content [45,46].

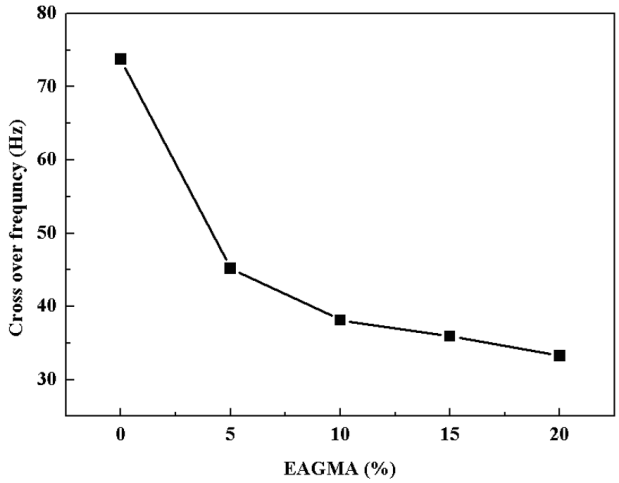

Fig.6. Curves of crossover frequency versus content of EAGMA for PEI/EAGMA blends.

Moreover, the Cole-Cole technique developed by Han [47] in which η" is plotted versus η' and is a useful tool to assess the compatibility of blends. As shown in Fig. 7, the PEI/EAGMA blends have only one circular arc in the curve, suggesting a homogeneous phase [48~50].

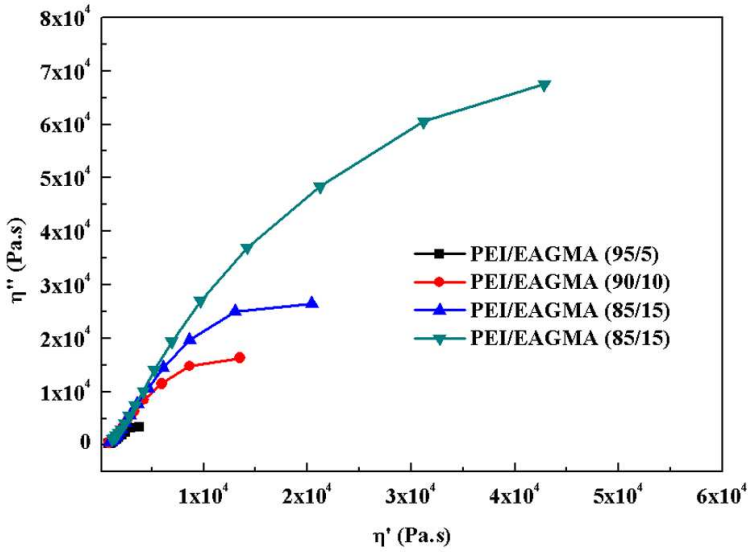

Fig.7. Cole-Cole plots for the PEI/EAGMA blends at 330 °C

3.4 Thermal property

The dynamic thermomechanical behavior and thermalstability of pure EAGMA, PEI and PEI/EAGMA blends were studied. The glass transition temperature (Tg), thermal degradation temperatures of 5 and 10% weight losses ($T_{5\%}$ and $T_{10\%}$) and the carbon yields at 800 °C of pure EAGMA, PEI and PEI/EAGMA blends were listed in Table 3. It can be seen, the Tg of EAGMA and PEI was -25 °C and 215 °C respectively, the Tg of the PEI/EAGMA blends was a little lower than PEI and decreases with increasing EAGMA content. Meanwhile, the thermal stability of the PEI/EAGMA blends decreases with increasing EAGMA content too.

Tab. 3 Thermal properties of EAGMA, PEI and PEI/EAGMA blends

EAGMA content (wt%)	0	5	10	15	20	100
T_g (°C)	215	210	206	201	198	-25
$T_{5\%}$ (°C)	538	488	465	456	451	418
$T_{10\%}$ (°C)	547	540	489	484	471	431
Carbon yield at 800 °C (%)	48.46	47.68	46.58	44.74	42.32	0.71

Moreover, the HDT of neat PLA and PEI/EAGMA blends were investigated. As seen in Fig.8, the EAGMA exhibit great effect on the HDT of PEI/EAGMA blends and the difference between the maximum value and the minimum value was 24 ^{o}C. It is well known that the thermal stability of elastomer is poor, so the introduction of EAGMA resin will decreases the HDT of PEI. Although the HDT of PEI/EAGMA blends decreases with the increasing EAGMA content, the minimum HDT still achieve 165 ^{o}C which is greatly higher than that of conventional plastics such as PP, PA66 and PC etc.

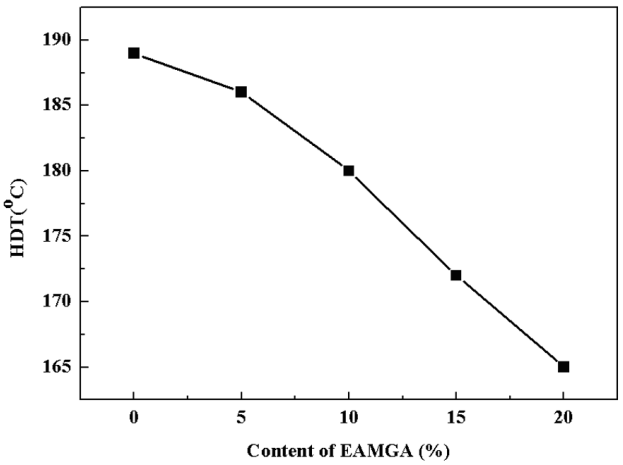

Fig.8. Curves of the HDT versus the content of EAGMA for PEI/EAGMA blends.

3.5 Mechanical properties

Fig.9 shows the mechanical properties of the PEI/EAGMA blends and microcellular foams with various EAGMA content. The tensile strength and flexural strength of PEI/EAGMA blends decrease from 102.7 MPa to 56.5 MPa, and 146.6 MPa to 90.7 MPa as the content of EAGMA increased from 0 to 20 wt %, respectively. Corresponds to the morphology analyses in section 3.1, the introduction of EAGMA increases the toughness of PEI. The maximum values of notched charpy impact

strength were observed in the 20 wt% EAGMA–introduced PEI/EAGMA blends, where about 27.9 KJ/m^2 4-5 times higher than that of pure PEI. The results indicate that the EAGMA has good toughening effects on PEI matrix. The mechanical properties of microcellular PEI/EAGMA foams exhibited similar trend with that of unfoamed PEI/EAGMA blends. The tensile strength and flexural strength of microcellular PEI/EAGMA foams decrease from 77.9 MPa to 46.3 MPa, and from 136.7 MPa to 72.53 MPa as the content of EAGMA increased from 0 to 20 wt %, respectively, and the notched charpy impact strength of microcellular PEI/EAGMA foams reaches to 10.2 KJ/m^2. The mechanical properties especially the notched charpy impact strength of microcellular PEI/EAGMA foams are obviously lower than that of unfoamed PEI/EAGMA blends. Huang et al. [51] reported that the smaller the cell size is, the better mechanical properties are. It is probably that the cell size is still too big to prevent the expansion of the crack during the impact test.

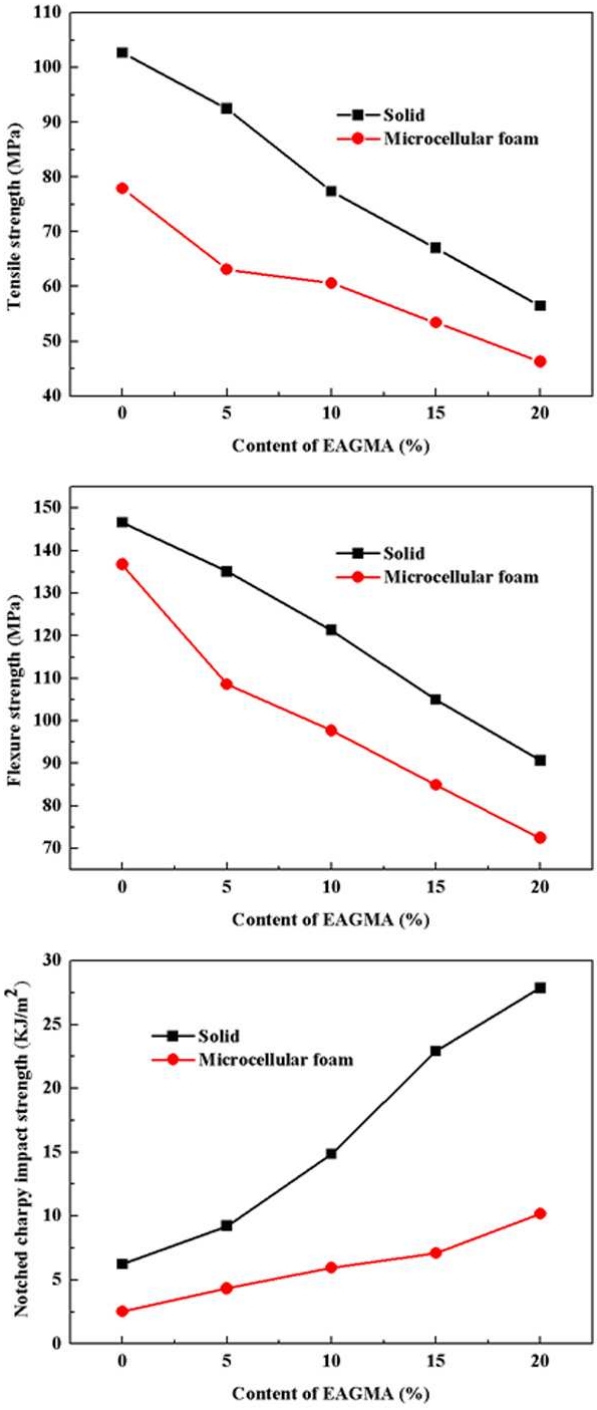

Fig.9. Curves of the mechanical properties versus the content of EAGMA for PEI/EAGMA blends and foams.

3.6 Cell properties

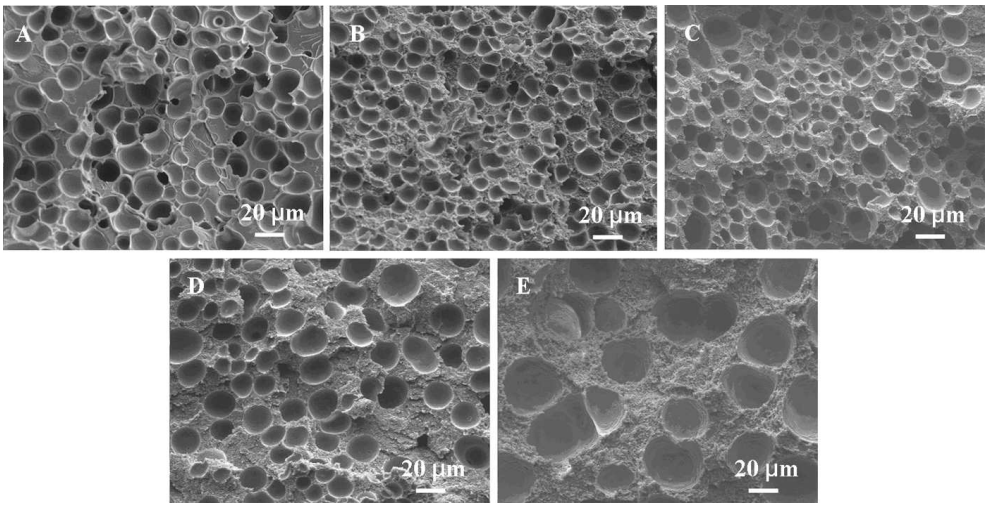

Fig. 10. SEM micrographs of microcellular PEI/EAGMA foams. (A) PEI/EAGMA=100/0; (B) PEI/EAGMA=95/5; (C) PEI/EAGMA=90/10;(D) PEI/EAGMA=85/15; (E) PEI/EAGMA=80/20.

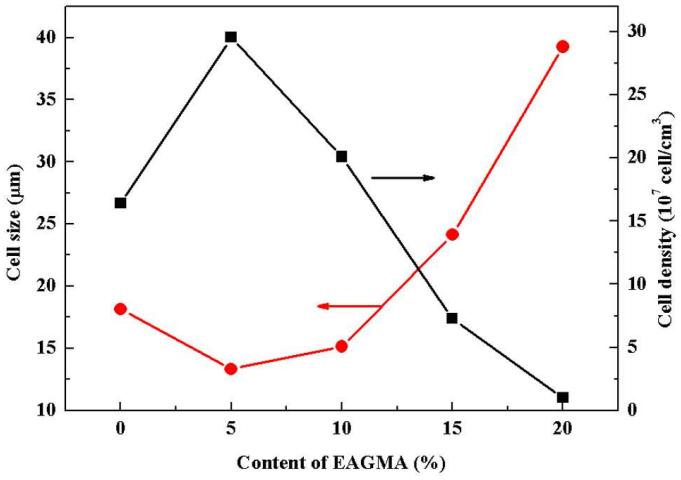

Fig. 11. Curves of the cell properties versus the content of EAGMA for microcellular PEI/EAGMA foams.

Fig.10 and Fig. 11 show the cell properties of microcellular PEI/EAGMA foams. Evidently, as the content of EAGMA increases, the cell size decreases to minimum value of 13.3 μm and then increases to maximum value of 39.3 μm. On the one hand,

with the increaseing EAGMA content the melt strength of PEI/EAGMA blends enhanced, so the cell coalescence reduced and the cell size decreased. On the other hand, the solubility of N_2 gas in arcrylic materials such as EAGMA is small [52], thus, with the growth of EAGMA content the N_2 solubility in PEI/EAGMA blends reduced that is to say the amount of N_2 gas which diffused from PEI/EAGMA melt increased. The diffusion of gas will lead to cell coalescence, so the cell size increased. Moreover, the decreasing solubility of N_2 gas in PEI/EAGMA blends lead to a dramatic reduction in cell density. As shown in Fig.12, the mass density of both foamed and unfoamed PEI/EAGMA was decreased with the increasing EAGMA content. And the two curves of mass density gradually approach with the increasing EAGMA content. The result indicates that the weight reduction of microcellular PEI/EAGMA foams decreases with the increasing EAGMA content. This phenomenon also confirm the analyses above that EAGAM plays an important roles of N_2 solubility in PEI/EAGMA blends.

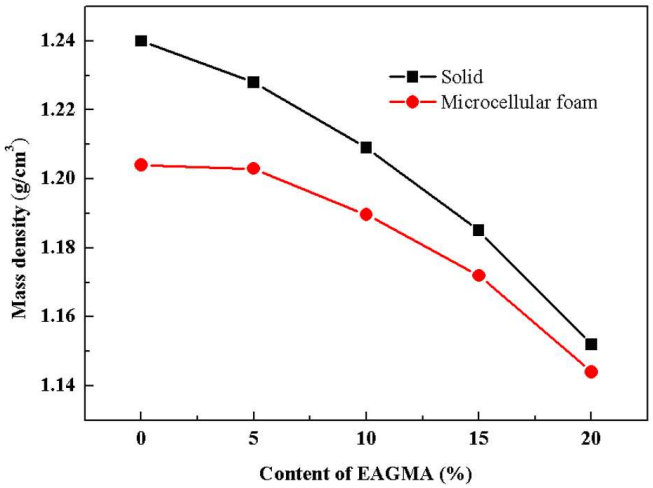

Fig.12. Curves of the mass denstiy versus the content of EAGMA for PEI/EAGMA blends and foams.

3.7 Dielectric property

Considering the application of microcellular foam,such as in electrical industry, the effects of EAGMA content and microcellular structure on the dielectric property of PEI/EAGMA have been studied. Fig. 13 shows the variation in dielectric constant ε' and dielectric loss tanδ with frequency in unfoamed PEI, EAGMA and microcellular PEI/EAGMA foam as a function of increasing EAGMA loading content. It can be seen obviously that the dielectric constant and loss of the materials can be effectively reduced through the technology of micro-foaming. As shown in Fig. 13(A), all the PEI/EAGMA foam has lower dielectric constant than that of unfoamed PEI and EAGMA, moreover, it is worth to note that the dielectric constant of the PEI/EAGMA foam increases with increasing EAGMA content. There are mainly two reasons for this phenomenon. Firstly, the dielectric constant of EAGMA is the highest, the more EAGMA the PEI/EAGMA foam contain, the higher dielectric constant it has. Secondly, the N_2 solubility in PEI/EAGMA blends reduced with the increase of EAGMA loading because of the solubility of N_2 gas in EAGMA is small, that is to say the more EAGMA the PEI/EAGMA blends has, the less gas the PEI/EAGMA foam contain, so the dielectric constant of microcellular PEI/EAGMA foam close to unfoamed PEI and EAGMA when EAGMA content increased.

From Fig 13(B) it can be seen that EAGMA has the highest dielectric loss but PEI is much lower, the dielectric loss of pure PEI foam was the lowest. Similarly, the dielectric loss of the PEI/EAGMA foam was between EAGMA and PEI and increased

with the increasing EAGMA content. Nevertheless, the dielectric loss of the PEI/EAGMA foam with 20 wt% EAGMA content is a little higher than PEI but much lower than that of EAGMA. The low dielectric constant and loss of PEI/EAGMA foam make them candidates for potential applications in electrical industry.

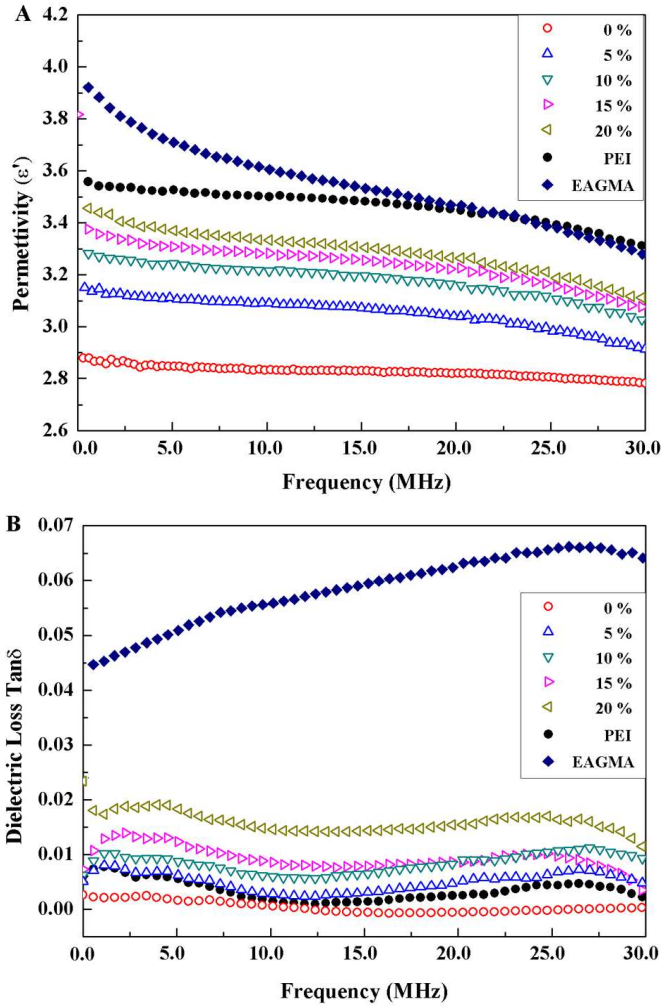

Fig.13. Dielectric property of unfoamed (closed symbols) PEI, EAGMA and PEI/EAGMA foams with various EAGMA content.

4 Conclution

In conclusion, EAGMA exhibits excellent toughening effect in the PEI/EAGMA system. The notched charpy impact strength of PEI/EAGMA blends with 20 wt% EAGMA is 27.9 KJ/m^2 which is 4~5 times higher than that of pure PEI. The

compatibility between PEI and EAGMA is great and the molecular mobility of PEI can be restricted by EAGMA. Moreover, EAGAM plays an important role in the microcellular structure of PEI/EAGMA foam and its final dielectric property. The dielectric constant and loss of the materials can be effectively reduced through the technology of micro-foaming. The PEI/EAGMA foam with high thoughness, low dielectric constant and dielectric loss is believed to have potential application in many areas such as electrical industry .

References

[1]. Martini JE, Waldman FA, Suh NP (1982) SPE ANTEC'82.

[2]. Martini JE, Suh NP, Waldman FA (1984) U. S. Patent 4,473,665.

[3]. Seeler KA, Kumar V (1993) J Reinf Plast Compos 12: 359.

[4]. Baldwin DF, Park CB, Suh NP (1996) Polym Eng Sci 36: 1437.

[5]. Baldwin DF, Park CB, Suh NP (1996) Polym Eng Sci 36: 1446.

[6] Colton JS, Suh NP (1987) Polym Eng Sci 27:485-492.

[7] Baldwin DF, Park CB, Suh NP, (1996) Polym Eng Sci 36:1437.

[8] Shimbo M, Baldwin DF, Sun NP (1995) Polym Eng Sci 35:1387.

[9].Jenkins MJ, Harrison KL, Silva MMCG, Shakesheff KM, Whitaker MJ (2006) Eur Polym J 42:3145.

[10] Hwang SS, Liu SP, Hsu PP, Yeh JM, Chang KC, Lai YZ (2010) International Communications in Heat and Mass Transfer 37:1036.

[11] Yuan MJ, Turng LS, (2006) Polymer 46:7273.

[12]Pilla S, Kramschuster A, Yang LQ, Lee J, Gong SQ, Turng LS (2009) Mater Sci

Eng C 29:1258.

[13] Xu ZM, Jiang XL, Liu T, Hu GH, Zhao L, Zhu ZN, Yuan WK (2007) J Supercrit Fluids 41:299.

[14] Jiang XL, Liu T, Xu ZM, Zhao L, Hu GH, Yuan WK (2009) Journal of Supercrit Fluids 48:167.

[15] Krause B, Sijbesma HJP, Münüklü P, Van NFA, Wessling M (2001) Macromolecules 34:8792.

[16] Miller D, Chachaisucha P, Kumar V (2009) Polymer 50:5576.

[17]Miller D, Chachaisucha P, Kumar V (2011) Polymer 52:2910.

[18] Nemoto T, Takagi J, Ohshima M (2010) Polym Eng Sci 50:2408-2416.

[19] Arzak A, Eguiazabal JI, Nazabal J (1997) J Macromol Sci Phys B36:233.

[20] Harris JE, Robeson LM (1988) J Appl Polym Sci 35:1877.

[21] Frigione M, Naddeo C, Acierno D (1996) Polym Eng Sci 36:2119.

[22] Bicakci S, Cakmak M (1998) Polymer 39:4001.

[23] Crevecoeur G., Groeninckx G. (1991) Macromolecules 24:1190.

[24] Torre L, Kenny JM (1992) Polym Compos 13:380.

[25] Chun YS, Lee HS, Jung HC, Kim WN (1999) J Appl Polym Sci 72:733.

[26] Jenkins MJ (2000) Polymer 41:6803

[27] Jenkins MJ (2001) Polymer 42:1981.

[28] Chen JB, Guo Q, Zhao ZP, Wang XM, Duan CL (2012) Procedia Engineering 36:96.

[29] Chen JB, Guo Q, Zhao ZP, Shao XL,Wang XM, Duan CL (2013) J Appl Polym Sci 127:2220.

[30] Chen HL, Hwang JC, Wang RC (1998) Polymer 39:6067.

[31] Cakmak M, Kim JC (1997) J Appl Polym Sci 65:2059.

[32] Kim JC, Cakmak M, Zhou X (1998) Polymer 39:4225.

[33] Woo EM, Yau SN (1997) Macromolecules 30:3626.

[34] Chen HL, Hwang JC, Chen CC, Wang RC, Fang DM, Tsai MJ (1997) Polymer 38:2747.

[35] Vallejo FJ, Eguiazabal JI, Nazabal J (2001) Journal of Applied Polymer Scienc 80:885-892.

[36] Martinez JM, Eguiazabal JI, Nazabal J (1993) J Appl Polym Sci 48:935.

[37] Martinez JM, Eguiazabal JI, Nazabal J (1996) J Appl Polym Sci 62:385.

[38] Bastida S, Eguiazabal JI, Nazabal J (1996) Polymer 37:2317.

[39] Bastida S, Eguiazabal JI, Nazabal J (1996) Eur Polym J 32:1229.

[40] Qipeng G, Lingwei Q, Mengxian D, Zhiliu F (1992) Eur Polym J 28:1045.

[41] Choi KY, Lee SG, Lee JH, Liu J (1995) Polym Eng Sci 35:1643.

[42] Chandra A, Gong SQ, Turng LS (2005) Polym. Eng. Sci. 45:52.

[43] Lee ST (2000) CRC, Lancaster.

[44] Wu S (1982) New York: Marcel Dekker.

[45] Yousef JJ (2010) Vinyl Additive Technol 16:70.

[46] Gahleitner M (2001) Prog Polym Sci 26:895.

[47] Han CD, Lem KW (1983) Polym Eng Rev 12: 135.

[48] Chopra D, Kontopoulou M, Hatzikiriakos SG (2002) Rheol Acta 41:10.

[49] Palierne, JF (1990) Rheol Acta 29:204.

[50] Zheng Q, Du M, Yang B, Wu G (2001) Polymer 42:5743.

[51] Huang HX, Wang JK (2008) Material properties 27:513.

[52] Gong S, Yuan M, Chandra A, Kharbas H, Osorio A, Turng LS (2005) International Polymer Processing, 20: 202.

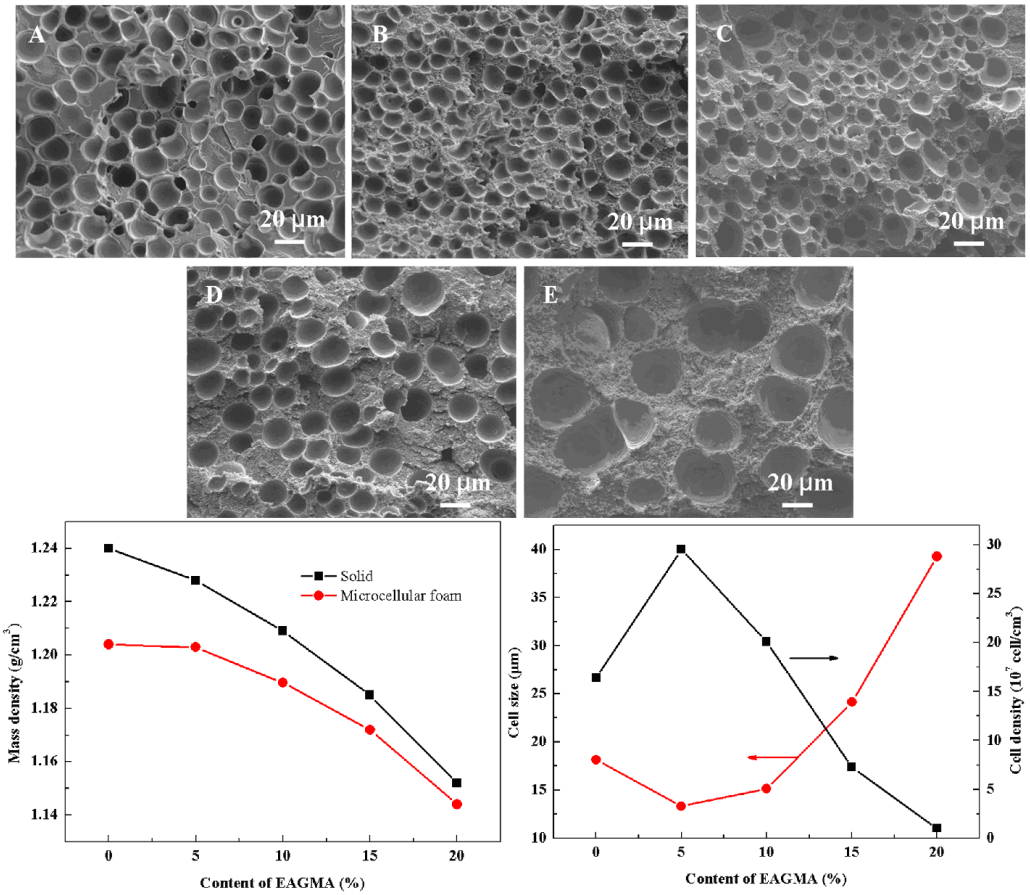

EAGAM plays an important role in the microcellular structure formation and had excellent toughening effect in the PEI/EAGMA system.